

Acoustically induced transparency by using concentric spherical shells with coaxial aperture array

Cite as: Appl. Phys. Lett. **109**, 073503 (2016); <https://doi.org/10.1063/1.4961504>

Submitted: 19 June 2016 . Accepted: 10 August 2016 . Published Online: 17 August 2016

Guan Wang, Li Jin, Peng Li, and Zhuo Xu



View Online



Export Citation



CrossMark

ARTICLES YOU MAY BE INTERESTED IN

[Acoustically induced transparency using Fano resonant periodic arrays](#)

Journal of Applied Physics **118**, 164901 (2015); <https://doi.org/10.1063/1.4934247>

[Acoustic metasurface-based perfect absorber with deep subwavelength thickness](#)

Applied Physics Letters **108**, 063502 (2016); <https://doi.org/10.1063/1.4941338>

[Acoustic superlens using Helmholtz-resonator-based metamaterials](#)

Applied Physics Letters **107**, 193505 (2015); <https://doi.org/10.1063/1.4935589>

Lock-in Amplifiers
up to 600 MHz



Watch



Acoustically induced transparency by using concentric spherical shells with coaxial aperture array

Guan Wang,¹ Li Jin,^{1,a)} Peng Li,^{2,3} and Zhuo Xu^{1,a)}

¹*Electronic Materials Research Laboratory, Key Laboratory of the Ministry of Education and International Center for Dielectric Research, Xi'an Jiaotong University, Xi'an 710049, China*

²*Department of Mechanical Engineering, Hong Kong Polytechnic University, Hong Kong, People's Republic of China*

³*School of Human Settlements and Civil Engineering, Xi'an Jiaotong University, Xi'an 710049, People's Republic of China*

(Received 19 June 2016; accepted 10 August 2016; published online 17 August 2016)

An acoustically induced transparency device based on Fano resonance was designed and fabricated. The proposed design ensures excitation and interference of two associated resonance modes by locating the concentric shells with apertures. The inserted shell generates the destructive interference resonance to the original resonance. Numerical simulations and experiments demonstrate that this designed structure could generate Fano resonance and can be used to generate acoustically induced transparency with potential applications in nonlinear enhancement devices and sensing. *Published by AIP Publishing.* [<http://dx.doi.org/10.1063/1.4961504>]

Electromagnetically induced transparency (EIT) is a phenomenon specific to periodic media, in which both the electromagnetic fields and the material states are modified. EIT generates a sharp window transparency associated with steep dispersions in optics and photonics,^{1–3} which is due to the quantum destructive interference of the different exciting modes in a three-level atomic system.⁴ The peculiar properties of EIT have been utilized to enhance nonlinear frequency conversion,^{5–8} reduce the group velocity of light,^{9–11} and freeze the light.¹² Recently, classical analogies of EIT based on resonant coupling have been demonstrated in optical resonator coupling^{13–18} or metamaterial structure coupling.^{19–23} In particular, the EIT phenomenon in metamaterials by periodic structure coupling has attracted much attention to controlling the electromagnetic wave in device miniaturization.^{24,25} Some studies have reported the generation of an EIT effect for the active control of the wave propagation in the THz range by using MEMS and coupled metamolecules^{26,27} and generation of ultrahigh-quality Fano resonances in the asymmetry regime range.²⁸ Some study demonstrated the Induced Transparency by the latticed unit.²⁹ The arrangement of the unit and the number of layers are influence factors on the transmission curve at propagation directions.^{30–34} Up to date, there have been few studies related to acoustically induced transparency (AIT) by analogy to electromagnetics, although the equations governing acoustic waves are equivalent to the Maxwell equations for electromagnetic waves in two-dimensional (2D) periodic structures. Existing works on AIT have focused on generating AIT by using resonances coupled with different Q-factors,³⁵ detuned acoustic resonators (DARs),¹⁰ or coaxial bottom-closed pipe pair.³⁶ Fano Resonance is a resonant scattering phenomenon caused by multi-resonance coupling.^{16,37,38} The acoustic Fano resonance is generated by the coupling of the highly localized trapped modes,^{37,39} which in sharp contrast to the inductive–capacitive resonance becomes

extremely sensitive to the conducting properties of the resonators. The induced transparency is generated by coupling of the two atomic resonances in a three-level atomic system. Therefore, the acoustic Fano resonance can be used to generate the induced transparency in the acoustic domain. In this paper, an acoustic structure device supporting Fano resonance and AIT characteristics is designed and fabricated. Specifically, this acoustic device expands the application of the induced transparency effect from electromagnetics to acoustics. Moreover, it could generate Fano resonance and can be employed to generate acoustically induced transparency.

The structure is a 2D plane periodic array of subwavelength unit cells, which is composed of concentric spherical shells with coaxial apertures. The property of the spherical shell is a rigid acoustic material which ensures that the cavity resonance is a unique resonance source and ignores the structure deformation. The resonance frequency of the spherical shell with an aperture depends on the cavity of the shell and the size of the opening aperture.⁴⁰ The resonance frequency can be expressed approximately as $f = \frac{c}{2\pi} \sqrt{\frac{S}{l_{eff}V}}$; here, c is the sound velocity in the surrounding environment, S is the cross area of the aperture, l_{eff} is the effective thickness of the aperture neck, and V is the column of the shell cavity, respectively.⁴¹

Figure 1 illustrates the schema of the designed array excited by acoustic waves. The cell of the array is composed of concentric spherical shells with coaxial apertures. Other shapes of cavities are also possible, but the spherical shell is considered in this case because of its low reflection and strong localized resonance.

Figure 2(a) depicts the transmittance of the single resonance structure excited by a normal acoustic wave and labels the geometrical parameters. The material property of the structure is featured by a rigid acoustic material for generating the localized Helmholtz resonance, which depends on the cavity of the shell and the size of the cross area of the aperture. In these figures and the following text, the geometrical parameters r , t , α , and a represent the radius of the shell,

^{a)} Authors to whom correspondence should be addressed. Electronic addresses: ljin@mail.xjtu.edu.cn and xuzhuo@mail.xjtu.edu.cn

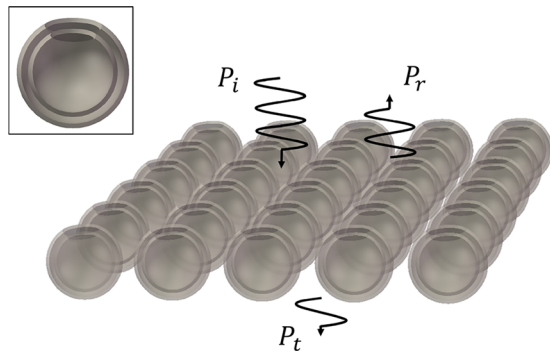


FIG. 1. The schema of the designed array excited by acoustic waves. The incident wave P_i passing through the array generates the reflect wave P_r and the transmission wave P_t .

the thickness of the shell, the opening angle of the aperture, and the lattice constant as could be seen in Fig. 2(a), respectively. An acoustic plane wave is normal incident to the aperture of the shell shown in Fig. 1(c). Here, transmittance is defined as $|T|^2$, where $|T|$ is the amplitude of the transmitted pressure under the excitation by a unit amplitude plane wave. Fig. 2(a) clearly demonstrates that the transmittance curve can be considered as a symmetric Lorentzian curve, which is attributed to Helmholtz resonance excited by acoustic waves. Helmholtz resonance can be considered as a basic resonance mode for interference resonances.⁴² The resonance frequency of this resonance mode approximates 2900 Hz. Fig. 2(b) shows the acoustic pressure distribution of the cross section across a single spherical shell at the resonance frequency marked in Fig. 2(a). As there is only one aperture on the shell, a strong localized resonance in the shell's cavity should be generated. Close to the resonance frequency, it should generate a fierce interference between the incident and the scattered waves at the aperture. At the resonance frequency, the incident wave and the scattered wave should generate a stalemate at the aperture, while the energy of the acoustic wave should be locked in the spherical shell, as illustrated in the acoustic pressure field distribution in Fig. 2(b).

To obtain the expected AIT effect, it is necessary to introduce another resonance to break the existing resonance. The primary aim of the following study is to generate interference of the two resonance modes required by the Fano resonance and AIT effect by using two concentric shells with apertures.

The symmetric Lorentzian resonance changes to an asymmetric Fano resonance by inserting another resonance mode, which consists of two concentric spherical shells with apertures. Meanwhile, the previous resonance mode should be regulated by the inserted resonance mode for the AIT effect. The coupling of the two resonance modes associated with each spherical shell with an aperture results in the Fano resonance and AIT effect in the response of a 2D array of this concentric spherical shell structure.

The periodic array of the concentric spherical shell structure is illustrated in Fig. 1(a). The radiuses of the outer shell and the inner shell are r_1 and r_2 , thicknesses of the two shells are $t_1 = t_2 = t$, and the same opening angles of the aperture are $\alpha_1 = \alpha_2 = \alpha$. Therefore, the gap between the two shells and the space of the inner shell generate two inter-ferential acoustic resonance modes. The shared area of the apertures should be the interference zone of the two resonance modes.

The transmittance of the array of the concentric spherical shell structure exhibited in Fig. 3(a) is excited by an acoustic plane wave. In this case, the transmittance shows that a peak between the two resonance valleys resembles opening a window, which indicates the existence of the AIT effect due to the interference between the two resonances. Figs. 3(b)–3(d) show the pressure field distribution across the sections of the shells at the resonance modes in Fig. 3(a).

Fig. 3(b) is exactly at the first resonance frequency point, and the acoustic pressure fields are confined inside the gap only. Also at this resonance frequency point, both shells interfere constructively leading to a restraint of transmittance or an enhancement of reflectance, as there is no absorption by the periodic array structure made of a completely rigid acoustic material. There is a dramatic increase in transmittance indicating the nonlinear enhancement region since the interference between the two modes takes place. This sharp increase caused by destructive interference is attributed to nonlinear enhancement in AIT. It is significant to note that the interval between points I and II generates a highly dispersive medium for slow sound behavior. Finally, the marked point III corresponds to the resonance of the inserted shell and the pressure fields are confined in the inner shell as shown in Fig. 3(d). Moreover, the interference of the two acoustic resonance modes in the range between marked points I and III generates an asymmetric curve attributed to Fano resonance.

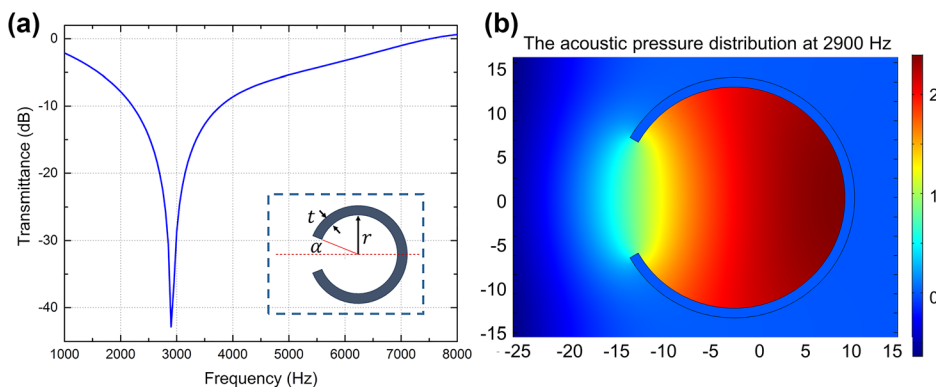


FIG. 2. (a) Transmittance of the single shell with one aperture array excited by a normal acoustic wave. (b) The acoustic pressure distribution of the cross section across a single shell at the resonance frequency.

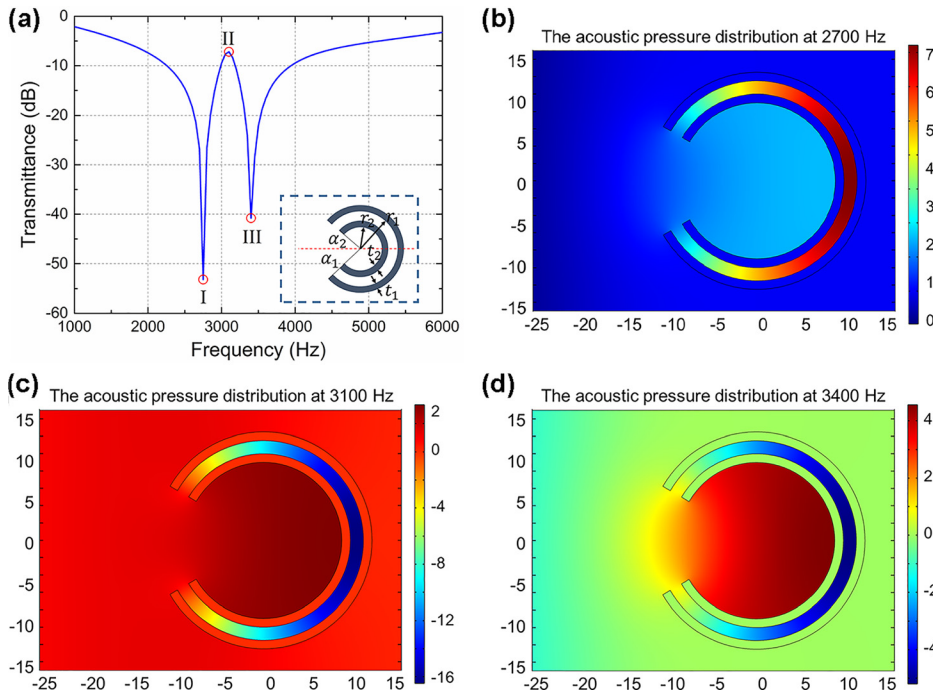


FIG. 3. (a) Transmittance of the concentric spherical shells with apertures. (b), (c), and (d) show the pressure distribution at the resonance frequency I, II, and III, viewing at the cross section.

Due to the inserted concentric shell for the Fano resonance and AIT effect, the relative positions become the influence factors apart from the previous structure effect. Fig. 4 illustrates the influence of transmittance by the relative position and angle of the two concentric shells. The relative position of the two concentric shells is expressed by $\Delta r = r_1 - r_2$, the gap between the two shells. In this case, the radius of the inner shell r_2 is reduced while the outer shell radius r_1 and thicknesses t are kept constant. To illustrate, altering r_2 directly affects the inserted resonance frequency, which increases with the decline of the radius of the inner shell. Meanwhile, the gap between the two shells Δr increases with the declining of r_2 , and the range of the two resonances broadens, as shown in Fig. 4(a). Fig. 4(b) illustrates the influence of the transmittance by the relative angle of the two concentric shells. It keeps the two shell shapes invariant and rotates the inner shell in the vertical plane, where the relative angle is expressed as $\Delta\alpha = \alpha_1 - \alpha_2$. Because of rotating the inner shell, there is a displacement in the two apertures. With the relative angle increasing, the coupling phenomenon is trailing off. When the relative angle is $\Delta\alpha > 30^\circ$, the

coupling phenomenon is discrete. The displacement between the two apertures brings a cavity between the two resonators; thus, another resonance mode is brought in as could be seen in Fig. 4(b).

The fabricated structure consists of two concentric spherical shells with apertures, as illustrated in Fig. 5 by 3D printing technology. To meet the dimensions of a standard measurement system for acoustic pressure, there is a cyclic belt around the structure to maintain the sample location in the center of the measured tubes. The measurement system is carried out using a 4206 series Transmission Loss Tube Kit produced by Brüel and Kjær Company. The two concentric spherical shells are kept at their concentric location by using a cylinder at the opposite side of the aperture to maintain the location. The cylinder connector can reduce the scattering in the spherical cavity, and other types of connecting shapes are also acceptable. The dimensions of the structure are $r_1 = 12.5$ mm and $r_2 = 10$ mm as the thickness of the array is equal to one quarter of the target sound wave. Thicknesses of the shells are $t_1 = t_2 = 1$ mm, and the angles of the apertures are $\alpha_1 = \alpha_2 = 30^\circ$. Fig. 5(a) plots transmittance through the sample via the measurement system.

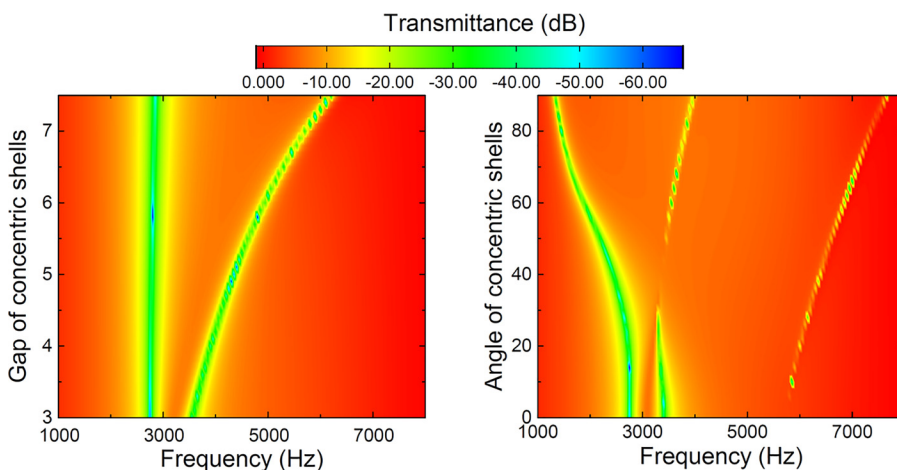


FIG. 4. (a) The spectrum of transmittance, through the array of the two shell resonators of varying the radius of the inner shell, where all the other parameters are kept invariant. (b) The spectrum of transmittance, through the array of the two shell resonators of varying the cross angle $\Delta\alpha$ of the two shells, where all the other parameters are kept invariant.

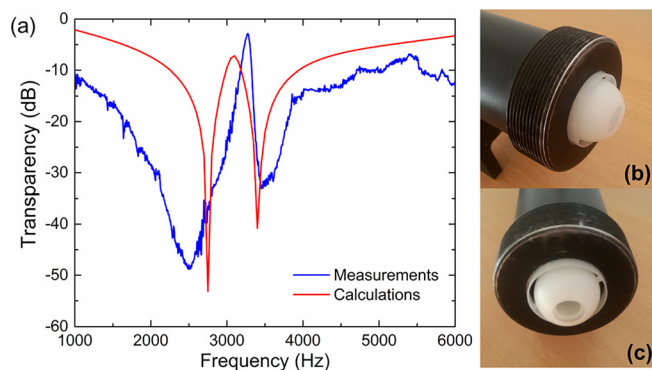


FIG. 5. Experiment measured transmittance through the designed array exhibiting the AIT effect. There is a window transparency as predicted.

There are two strong attenuations observed in the transmittance spectra, and an AIT phenomenon resembles a peak in transmittance spectra between the two attenuations. The two attenuations reach more than -40 dB around the resonance frequency. The AIT window effect appears near 3100 Hz, with transmittance reaching -5 dB between the two attenuations.

A periodic array of the subwavelength multi-resonator structure, which supports and demonstrates the Fano Resonance and AIT effect, has been designed and fabricated. This research systematically investigates the mechanism of sound resonance in the concentric spherical shells array and illustrates the relationship between transmittance and relevant geometrical parameters. By drawing on 3D printing technology for prototyping and verifying, Fano resonance and the AIT phenomenon are measured and the corresponding results agree with previous predictions. This proposed strategy will definitely open up possibilities for designing and fabricating more practical AIT devices in the field of acoustic wave control applications.

This work was supported by the Natural Science Basis Research Plan in Shaanxi Province of China (Grant No. 2015JM5199), the Fundamental Research Funds for the Central Universities, the National Basic Research Program of China (973 Program) under Grant No. 2015CB654602, and “111” Project (Grant No. B14040).

¹S. E. Harris, *Phys. Today* **50**(7), 36 (1997).

²M. Fleischhauer, A. Imamoglu, and J. P. Marangos, *Rev. Mod. Phys.* **77**, 633 (2005).

³N. Liu, L. Langguth, T. Weiss, J. Kastel, M. Fleischhauer, T. Pfau, and H. Giessen, *Nat. Mater.* **8**, 758 (2009).

⁴X. J. Liu, J. Q. Gu, R. Singh, Y. F. Ma, J. Zhu, Z. Tian, M. X. He, J. G. Han, and W. L. Zhang, *Appl. Phys. Lett.* **100**, 131101 (2012).

⁵S. E. Harris, J. E. Field, and A. Imamoglu, *Phys. Rev. Lett.* **64**, 1107 (1990).

- ⁶A. Andre, M. Bajcsy, A. S. Zibrov, and M. D. Lukin, *Phys. Rev. Lett.* **94**, 063902 (2005).
- ⁷P. Tassin, T. Koschny, and C. M. Soukoulis, *Nonlinear, Tunable and Active Metamaterials* (Springer, 2015), p. 303.
- ⁸O. Wolf, A. A. Allerman, X. Ma, J. R. Wendt, A. Y. Song, E. A. Shaner, and I. Brener, *Appl. Phys. Lett.* **107**, 151108 (2015).
- ⁹J. Marangos, *Nature* **397**, 559 (1999).
- ¹⁰A. Santillan and S. I. Bozhevolnyi, *Phys. Rev. B* **84**, 064304 (2011).
- ¹¹M. Manjappa, S. Y. Chiam, L. Q. Cong, A. A. Bettiol, W. L. Zhang, and R. Singh, *Appl. Phys. Lett.* **106**, 181101 (2015).
- ¹²M. F. Yanik and S. H. Fan, *Phys. Rev. Lett.* **92**, 083901 (2004).
- ¹³H. Schmidt, K. L. Campman, A. C. Gossard, and A. Imamoglu, *Appl. Phys. Lett.* **70**, 3455 (1997).
- ¹⁴T. Opatrný and D. G. Welsch, *Phys. Rev. A* **64**, 023805 (2001).
- ¹⁵L. Maleki, A. B. Matsko, A. A. Savchenkov, and V. S. Ilchenko, *Opt. Lett.* **29**, 626 (2004).
- ¹⁶V. A. Margulis and M. A. Pyataev, *J. Phys.: Condens. Matter* **16**, 4315 (2004).
- ¹⁷W. J. Gu and Z. Yi, *Opt. Commun.* **333**, 261 (2014).
- ¹⁸Z. L. Duan, B. X. Fan, T. M. Stace, G. J. Milburn, and C. A. Holmes, *Phys. Rev. A* **93**, 023802 (2016).
- ¹⁹R. Singh, I. A. I. Al-Naib, Y. P. Yang, D. R. Chowdhury, W. Cao, C. Rockstuhl, T. Ozaki, R. Morandotti, and W. L. Zhang, *Appl. Phys. Lett.* **99**, 201107 (2011).
- ²⁰H. M. Li, S. B. Liu, S. Y. Liu, S. Y. Wang, G. W. Ding, H. Yang, Z. Y. Yu, and H. F. Zhang, *Appl. Phys. Lett.* **106**, 083511 (2015).
- ²¹S. Han, L. Q. Cong, H. Lin, B. X. Xiao, H. L. Yang, and R. Singh, *Sci. Rep.* **6**, 20801 (2016).
- ²²H. M. Li, S. B. Liu, S. Y. Wang, S. Y. Liu, Y. Hu, and H. B. Li, *Sci. Rep.* **6**, 21457 (2016).
- ²³K. A. Yasir and W. M. Liu, *Sci. Rep.* **6**, 22651 (2016).
- ²⁴E. Lheurette, *Metamaterials and Wave Control* (Wiley Online Library, 2013), p. 195.
- ²⁵S. A. Cummer, J. Christensen, and A. Alu, *Nat. Rev. Mater.* **1**, 16001 (2016).
- ²⁶P. Pitchappa, M. Manjappa, C. P. Ho, R. Singh, N. Singh, and C. Lee, *Adv. Opt. Mater.* **4**, 541 (2016).
- ²⁷L. Q. Cong, N. N. Xu, D. R. Chowdhury, M. Manjappa, C. Rockstuhl, W. L. Zhang, and R. Singh, *Adv. Opt. Mater.* **4**, 252 (2016).
- ²⁸Y. K. Srivastava, M. Manjappa, L. Q. Cong, W. Cao, I. Al-Naib, W. L. Zhang, and R. Singh, *Adv. Opt. Mater.* **4**, 457 (2016).
- ²⁹M. Manjappa, Y. K. Srivastava, and R. Singh, preprint [arXiv:1605.03277](https://arxiv.org/abs/1605.03277).
- ³⁰R. Sprik and G. H. Wegdam, *Solid State Commun.* **106**, 77 (1998).
- ³¹I. E. Psarobas and M. M. Sigalas, *Phys. Rev. B* **66**, 052302 (2002).
- ³²Y. Z. Wang, F. M. Li, K. Kishimoto, Y. S. Wang, and W. H. Huang, *Mech. Res. Commun.* **36**, 461 (2009).
- ³³Y. Z. Wang, F. M. Li, K. Kishimoto, Y. S. Wang, and W. H. Huang, *Eur. J. Mech. A-Solid* **29**, 182 (2010).
- ³⁴N. Aravantinos-Zafiris and M. M. Sigalas, *J. Vib. Acoust.* **135**, 041003 (2013).
- ³⁵F. M. Liu, M. Z. Ke, A. Q. Zhang, W. J. Wen, J. Shi, Z. Y. Liu, and P. Sheng, *Phys. Rev. E* **82**, 026601 (2010).
- ³⁶M. Amin, A. Elayouch, M. Farhat, M. Addouche, A. Khelif, and H. Bagci, *J. Appl. Phys.* **118**, 164901 (2015).
- ³⁷S. Hein, W. Koch, and L. Nannen, *J. Fluid. Mech.* **664**, 238 (2010).
- ³⁸R. Zafar and M. Salim, *IEEE J. Quantum Electron.* **51**, 7200306 (2015).
- ³⁹G. Yu and X. Wang, *J. Appl. Phys.* **115**, 044913 (2014).
- ⁴⁰R. C. Chanaud, *J. Sound Vib.* **178**, 337 (1994).
- ⁴¹M. Alster, *J. Sound Vib.* **24**, 63 (1972).
- ⁴²U. Fano, *Phys. Rev.* **124**, 1866 (1961).